

Highly Disaggregated Land Unavailability*

Chandler Lutz
Securities And Exchange Commission

Ben Sand
York University

Land Unavailability Data:
<https://github.com/ChandlerLutz/LandUnavailabilityData>

February 10, 2023

Abstract

We combine high-resolution satellite imagery with modern machine-learning methods to construct novel datasets that capture the geographic determinants of U.S. housing supply. This Land Unavailability (LU) measure is a markedly more accurate house price predictor than the popular proxy of [Saiz \(2010\)](#). We apply LU to fundamental housing finance problems to provide substantially more precise housing wealth elasticity estimates, new evidence on the relationship between house prices and entrepreneurship during COVID-19, and novel empirical tests of the supply-side speculation theory. Finally, our LU instrument is broadly uncorrelated with housing demand proxies, supporting its use as an instrument for house prices.

JEL Classification: R30, R31, R20;

Keywords: Land Unavailability, House Price Prediction, Buildable Land, Housing Market, Real Estate

*Lutz: lutzc@sec.gov. <https://chandlerlutz.github.io/>. Sand: bmsand@yorku.ca. <https://ben-sand.github.io/>. The Securities and Exchange Commission disclaims responsibility for any private publication or statement of any SEC employee or Commissioner. This article expresses the authors' views and does not necessarily reflect those of the Commission, the Commissioners, or other members of the staff.

1 Introduction

As housing is the largest financial asset for most households, economists often estimate the impact of house price fluctuations on broader outcomes. To do so, they typically employ an instrumental variable (IV) approach since reverse causality obfuscates the relationship between house prices and the variable of interest. The most popular such instrument, the [Saiz \(2010\)](#) elasticity IV, stems from supply-side constraints and combines land unavailable due to geographic building restrictions with local housing market regulations.¹

Yet [Guren et al. \(2021\)](#), henceforth GMNS) recently criticized the Saiz elasticity IV because it lacks predictive power for house prices. The low predictive power of the Saiz IV in the first stage of a two-stage least squares (2SLS) framework leads to imprecise estimates in the second stage, increasing uncertainty in the causal relationship between house price changes and other economic outcomes. In particular, the Saiz IV uses the land unavailable due to geographic constraints within a 50k km radius of each MSA's central city centroid. Yet cities vary drastically in size and shape, making the blunt Saiz method inappropriate for many cities. Indeed, a homogeneous approach across heterogeneous cities, for example, means that Saiz elasticity has relatively large coverage when cities are geographically small (e.g., the northeast) but relatively small coverage when cities are large (e.g., the southwest). [Davidoff \(2016\)](#) also dispraised the Saiz elasticity IV due to its potential correlation with local housing demand proxies, perhaps invalidating it as an instrument for house prices. Researchers face further constraints when using the Saiz IV. The Saiz data contain a small number of cities, just 273, compared to the Freddie Mac house price dataset used by GMNS, which has 380 cities, or the Zillow data, with over 800 cities. A smaller number of cross-sectional observations increases finite sample bias in 2SLS estimates. The Saiz data also use 1999 MSA/NECMA definitions, whereas most current housing datasets exploit modern

¹Several recent papers have employed the Saiz elasticity IV or land unavailability in their study of housing markets and the broader economy. For papers on the financial crisis, see [Mian and Sufi \(2009, 2011\)](#); [Mian et al. \(2013\)](#); [Mian and Sufi \(2014\)](#); [Griffin et al. \(2021\)](#). In entrepreneurship and firm formation, see [Adelino et al. \(2015\)](#). Other and related applications include [Chaney et al. \(2012\)](#); [Aladangady \(2017\)](#); [Baum-Snow and Han \(2020\)](#); [Tan et al. \(2020\)](#); [Büchler et al. \(2021\)](#); [Conklin et al. \(2021\)](#); [Gabriel et al. \(2021\)](#); [Gamber et al. \(2021\)](#); [Gupta et al. \(2021\)](#). For recent overviews of the drivers of house price cycles, see [Duca et al. \(2021\)](#); [Griffin et al. \(2021\)](#).

CBSA aggregations, perhaps creating measurement error as researchers must port the Saiz proxy to recent delineations.

To overcome these challenges, we construct new land unavailability (LU) estimates, with complete coverage of the contiguous United States at multiple levels of disaggregation down to zip codes. Our intent is to create plausibly exogenous, highly predictive proxies that researchers can use as instruments for house prices.

We extend the popular Saiz proxy in several directions. First, our data use more accurate satellite imagery that is now available from the United States Geographical Survey (USGS) with complete coverage of the contiguous U.S. We also recognize that cities are heterogeneous and that any specific LU proxy is likely measured with error. Thus, in constructing LU, we exploit modern machine-learning techniques to combine land unavailability estimates computed at multiple levels of disaggregation. The result is a comprehensive data-driven LU dataset that has strong predictive power for house prices. Within a 2SLS research design, our extensive geographic coverage and improved first stage fit (i) increases the precision of second stage estimates and (ii) allows for more granular fixed effects or controls that may buttress a causal interpretation of results.

Our overarching methodology spans housing datasets and econometric approaches. Broadly, the output is either a cross-sectional or panel LU-based house price instrument. The cross-sectional LU data are useful when the econometric equation of interest is in long differenced form (e.g., [Mian and Sufi \(2014\)](#) and equation 1 below), while the LU panel dataset is apt when the empirical setup employs panel data (e.g., GMNS and equation 2 below).

Specifically, we construct our land unavailability-machine learning instrument (the LU-ML IV) by combining land unavailability estimates via the performant XGBoost machine learning algorithm to predict house price growth out-of-sample. The XGBoost algorithm allows for local differences across geographies and non-linearities in the predictive relationship between land unavailability and house prices. The resulting out-of-sample predictions serve as an instrument for house prices.

Exploiting out-of-sample predictions bolsters the exogeneity of the LU-ML IV by ensuring

that it is independent of any local peculiarities that can contaminate an instrument. Indeed, the LU-ML IV comprises projections of the land unavailability–house price relationship onto each region based on data outside of that region. In this sense, the LU-ML IV builds on an extensive literature dating back to [Bartik \(1991\)](#) that projects national data onto ex ante local characteristics for instrument exogeneity.

We apply our comprehensive land unavailability dataset to three fundamental housing market problems to emphasize the various advantages of our LU measure. First, we re-estimate the key housing wealth elasticity regressions of [Mian and Sufi \(2014\)](#) and [Guren et al. \(2021\)](#). The LU-ML IV has superior geographic coverage compared to Saiz elasticity and, combined with machine-learning methods, yields notably more precise 2SLS estimates. Next, we further demonstrate the utility of the LU-ML IV approach in our study of house price growth and entrepreneurship during COVID-19. Third, we construct a novel index for buildable land that allows for new empirical tests of theoretical housing market hypotheses that were not previously possible with other data.

Our first application centers on re-estimating housing wealth elasticities. We start by demonstrating the efficacy of the LU-ML IV within the cross-sectional, long-differenced empirical specification of [Mian and Sufi \(2014\)](#). Specifically, Mian and Sufi show that falling housing net worth (HNW) caused large declines in non-tradable employment during the Great Recession via the equation

$$\Delta \log E_{i,2007-09}^{NT} = \alpha + \eta \cdot \Delta HNW_{i,2006-09} + \varepsilon_i \quad (1)$$

where $\Delta \log E_{i,2007-09}^{NT}$ is the 2007–09 log change in non-tradable employment for county i , proxied by either restaurant and retail employment (*Rest. & Retail*) or employment in industries with low geographic concentration (*Geog. Concen.*).² $\Delta HNW_{i,2006-09}$ is the 2006–09 change in housing net worth for county i .

Columns 1 and 2 of table 1 replicate the main result of [Mian and Sufi \(2014\)](#). As reverse causality obscures the causal relationship between changes in housing net worth and employment, Mian and Sufi instrument $\Delta HNW_{i,2006-09}$ with Saiz elasticity. The corresponding

²See [Mian and Sufi \(2014\)](#) for further information on these proxies for non-tradable employment.

first stage F -statistic is 11.07, and the first stage partial R^2 (the instrument's incremental contribution to the R^2) is 0.12, indicating that Saiz elasticity has moderate predictive power for changes in housing net worth. Columns 1 and 2 also only exploit data from 540 counties due to the limited geographic coverage of the Saiz IV, whereas the overall Mian and Sufi dataset contains 940 counties.³

Columns 3 and 4 re-estimate the main findings from [Mian and Sufi \(2014\)](#) using the LU-ML IV. These results highlight several advantages of our approach. Most importantly, first stage fit jumps with LU-ML IV: The first stage F -statistic increases 16 times, compared to regressions that use the Saiz IV, to 182.33, and the first stage partial R^2 rises fourfold to 0.48. High IV predictive accuracy in the first stage increases the precision of the second stage estimates. Indeed, when the instrument is the LU-ML IV, the standard errors on $\Delta HNW_{i,2006-09}$ fall between 33–54% for columns 3 and 4, compared to columns 1 and 2 that use Saiz elasticity. Last, notice that the number of observations (counties) grows substantially from 540 when using Saiz elasticity to 936 for the LU-ML IV, as the LU-ML IV has complete coverage for the contiguous United States. More observations reduce finite sample bias in 2SLS estimates. Altogether, the results in table 2 highlight the benefits of the LU-ML IV relative to previous approaches, especially in important research problems like understanding the causes of the sizable employment declines during the Great Recession.

Next, we document the utility of our panel-based LU-ML IV by re-estimating the housing wealth elasticity within the panel data setup of [Guren et al. \(2021\)](#) via the equation

$$\Delta y_{i,r,t} = \psi_i + \xi_{r,t} + \beta \Delta p_{i,r,t} + \Gamma X_{i,r,t} + \epsilon_{i,r,t} \quad (2)$$

$\Delta y_{i,r,t}$ is the log annual change in quarterly retail employment per capita (a consumption proxy in year-over-year first-difference form) for CBSA i in census region r at time t . Similarly, $\Delta p_{i,r,t}$ is the log annual change in quarterly house prices for CBSA i . The coefficient of interest, β , measures the housing wealth elasticity. ψ_i , $\xi_{r,t}$, and $X_{i,r,t}$ represent CBSA fixed effects, census region \times time fixed effects, and other controls, such as industry shares,

³MSAs are an aggregation of counties. Thus, as noted above, the 273 1999 MSAs/NECMAs with a Saiz elasticity estimate are mapped to 540 counties in the Mian and Sufi dataset.

respectively.⁴

Table 2 previews the estimation results from equation 2 and presents 2SLS estimates of housing wealth elasticities from 1978–2017. Column 1 replicates GMNS and uses Saiz elasticity as an instrument for house prices.⁵ Notice first in table 2 that the Saiz data contain just 270 CBSAs versus the 380 available in the broader GMNS dataset, highlighting the limited cross-sectional coverage of the Saiz IV. The Saiz elasticity IV also has only modest predictive power for house prices, with a first stage F -statistic of 14.37 and a first stage partial R^2 of 0.02.⁶ The second stage housing wealth elasticity estimate is statistically insignificant with a relatively large standard error.

The findings in column 2 that instead use the LU-ML IV are noteworthy. To start, first stage predictive power rises substantially: The first stage partial R^2 increases by a factor of six, relative to the Saiz IV in column 1, and the first stage F -statistic rises to 187.7. This jump in first stage fit leads to markedly more precise second stage estimates, with the 2SLS standard error falling from 0.54 in column 1 (Saiz elasticity) to 0.019 in column 2 (LU-ML IV). Together, these results highlight the key advantages of the LU-ML IV: Comprehensive geographic coverage and more accurate first stage predictions that allow for more granular controls and lead to lower second stage standard errors.

Our second application examines the impact of house price growth on entrepreneurship and self-employment during COVID-19. In this context, we also investigate media narratives indicating that the pandemic sparked an increased interest in entrepreneurship, via the housing channel, by comparing house price growth-induced entrepreneurship rates during the pandemic to those from the 2010s.⁷ Our approach builds on Adelino et al. (2015), who study the effects of house price growth on entrepreneurship and self-employment during the 2000s housing boom using Saiz elasticity as an instrument for house prices. We instead use

⁴See Guren et al. (2021) for a full list of controls.

⁵To use Saiz elasticity (a cross-sectional dataset) within a panel setup, GMNS multiply the Saiz elasticity proxy for each city by national-level house prices.

⁶Since Saiz elasticity has low predictive power, Guren et al. also develop a sensitivity instrument discussed in section 4.

⁷See “How Covid Inspired a New Generation of Entrepreneurs.” *Bloomberg News*. June 1, 2021. “Start-Up Boom in the Pandemic Is Growing Stronger.” *New York Times* August 19, 2021. “Over 5 Million New US Startups Show Covid-Era Boom Has Legs.” *Bloomberg News*. January 17, 2023.

the LU-ML IV since it affords a markedly larger dataset comprising over 1,000 counties and has substantially stronger predictive power for house prices.

We first find that the results of Adelino et al. extend to the COVID-19 pandemic: Local house price appreciation increased the number of small firms (those with less than 5 employees) but had little effect on the number of larger firms. In an extension of Adelino et al., estimates also indicate that the house price growth-entrepreneurship relationship strengthened sharply during the pandemic (2020Q2 - 2022Q2), relative to the pre-pandemic period (2011Q1 - 2020Q1), congruent with media narratives ascribing increased entrepreneurship to changing household preferences toward work during COVID-19.

Our last application uses satellite imagery to construct a new dataset that precisely measures the amount of buildable land in 2001 within a geographic polygon. Buildable land is the amount of land available for development after removing existing development, steep sloped terrain, water, wetlands, and parks. In a sense, buildable land is the complement to LU but also accounts for previous construction and parks. We then use this dataset to empirically test the land supply-side speculation theory of [Nathanson and Zwick \(2018\)](#).⁸ This theory posits that homebuilders during the 2000s boom viewed traditionally elastic housing markets with intermediate amounts of available land (e.g., Las Vegas and Phoenix) as potentially inelastic in the long run. Homebuilders then proceeded to bid up the prices of land in these intermediate markets, and, as land is a crucial input for home construction, prices increased as well. While [Nathanson and Zwick \(2018\)](#) provide anecdotal evidence supporting their theory, they could not perform formal statistical tests as no comprehensive buildable land dataset was previously available. In this paper, we undertake such tests and find that housing markets with intermediate amounts of buildable land experienced larger house price booms during the 2000s, relative to those with smaller or larger quantities of buildable land, congruent with the supply-side speculation theory.

Finally, we examine the correlation between LU and housing demand proxies, as using

⁸Note that an extensive literature studies the causes of the 2000's housing crisis and Great Recession. For an overview, see [Foote et al. \(2021\)](#) and [Griffin et al. \(2021\)](#). Here, we use this application to further demonstrate the utility of our data.

land unavailability as an IV depends on its exogeneity relative to demand factors. Criticisms of deploying land unavailability as an IV contend that it is positively correlated with housing demand factors related to amenities, the economics of agglomeration associated with higher education, and labor demand shocks ([Davidoff, 2016](#)). Davidoff further asserts that the impact of these factors has increased over time and thus will not be differenced out in a standard long-differenced regression.

Yet previous attempts to assess the exogeneity of land unavailability suffer from an intrinsic sample selection issue. The only other land unavailability proxy from [Saiz \(2010\)](#) used a small set of MSAs. As MSA qualification requires a population of 50,000 and as land unavailability increases the cost of construction, high land unavailability cities in the Saiz dataset are by definition associated with higher productivity, relative to similarly high land unavailability areas not associated with an MSA. Moreover, the Saiz data include just 273 of the 331 available 1999 MSAs/NECMAs. In other words, the MSAs in the Saiz data have limited coverage of the U.S. and represent a biased sample. Conversely, we use land unavailability data that spans the contiguous United States at multiple levels of aggregation and find that LU is largely unrelated to various housing demand factors. These results support using LU as a candidate instrument for house prices.

We further note that researchers can circumvent Davidoff's criticisms by including city-level fixed effects in a panel data structure where the dependent and endogenous variables are differenced (e.g., equations [2](#) and [3](#)). In that case, the fixed effects account for differential long-run trends across cities over the sample period and thus the primary concern in [Davidoff \(2016\)](#). Last, we caveat this discussion by noting that the exogeneity of any instrument, including the LU-ML IV, depends on the econometric setup, the dependent and endogenous variables, controls, and the time period employed. Thus, we encourage researchers to pursue exogeneity assessments within the context of each study's research design.

2 Data

The United States Geographical Survey (USGS) builds the two primary datasets necessary to measure land unavailability due to steep sloped terrain, water, and wetlands.⁹ The first is the USGS National Elevation Dataset (NED) 3DEP 1 arc-second Digital Elevation Model (DEM). The 1 arc-second DEM data provide continuous coverage of the United States at approximately a resolution of 30 meters. The original Saiz dataset uses lower resolution 3 arc-second DEM data with a resolution of approximately 90 meters. The DEM data allow us to calculate slope files and hence the percentage of land unavailable due to a steep slope. Our second main dataset is the USGS 2011 Land Cover dataset. These data use LandSat imagery to classify land use in the U.S. The relevant categories for land unavailability are water (oceans, lakes, rivers, etc.) and wetlands. LandSat imagery also provides the basis for our buildable land dataset. Finally, we incorporate other geospatial data, such as shapefiles for various geographies from the U.S. Census Bureau and satellite imagery from Google Maps.

2.1 Other Data

Our data also include several essential housing and economic variables. House prices are from Freddie Mac or Zillow. The BLS Quarterly Census of Employment and Wages (QCEW) provides employment by industry and county and firm counts by employee size. We tabulate zip code household income and household counts from the IRS Statistics of Income. Business payrolls, employment, and establishment counts at the zip code level are from the Census County Business Patterns. From the 2000 U.S. Census at the zip code level, we retain the percentage of people with a college education and the share of foreign born. Data also span a zip code amenities index that aggregates information on access to restaurants and bars, retail shopping, public transit, and other amenities. The Missouri Data Bridge provides a geographic correspondence engine to crosswalk data across geographies. Last, data for our housing wealth elasticity applications are from Mian and Sufi (2014) and Guren et al. (2021).

⁹<https://www.usgs.gov/the-national-map-data-delivery>

3 Land Unavailability and the Construction of the LU-ML IV

The groundbreaking work of [Saiz \(2010\)](#) provides the foundation for this paper, as it was the first to use satellite imagery and GIS methods to compute proxies of land unavailability. Saiz starts by using the USGS 90 meter DEM data to calculate the percentage of land unavailable due to a steep slope. Specifically, he notes that land with a gradient above 15 percent faces architectural impediments to construction. The second dataset that Saiz employs is the 1992 Land Cover dataset. This latter dataset, combined with digital contour maps, measures the percentage of unavailable land due to oceans, lakes, rivers, etc. Combining these two sources, Saiz computes the share of land unavailable for construction (due to steep sloped terrain, water, and wetlands) within a 50k kilometer (km) radius around the centroid of each MSA's first central city using 1999 MSA/NECMA definitions.

As an example of the Saiz approach, figure 1 plots Google satellite imagery for the Los Angeles-Long Beach MSA using the 1999 delineations of [Saiz \(2010\)](#). The blue outlined area represents the Los Angeles-Long Beach MSA polygon boundary, the orange polygons signify the central cities (Los Angeles, Long Beach, Pasadena, and Lancaster), the red dots are the central city centroids, and the yellow circle has a 50k km radius around the first central city centroid (in this case, the Los Angeles central city). Saiz uses the area within the yellow circle to calculate land unavailability. Clearly, the location of the first central city centroid determines the geography used in the Saiz calculation: The yellow circle in figure 1 captures Los Angeles proper but does not cover the central city around the Lancaster and Palmdale areas, two cities with a combined 2000 population of over 230,000, or eastern Los Angeles. In the greater LA area, these are the exact regions where much of the new construction occurs. Moreover, Anaheim and Irvine, two cities in south LA often included as a part of LA in the modern CBSA definitions used by many housing datasets, are also left out of the Saiz circle. Last, the Saiz circle does not cover the disjointed polygons representing the Catalina islands.

Generally, the Saiz circles undercover MSAs that span large geographic areas but cover more land area for comparatively smaller polygons (noting again that every Saiz circle has a 50k km radius around the central city centroid). Larger MSAs are typically in the southwest,

while those in the northeast are usually smaller. Thus, the coverage of the Saiz circles correlates with geography. Cities are also heterogeneous along other dimensions, such as the shape of their polygons or their location relative to other cities. Therefore, as noted by GMNS, Saiz applies a blunt, homogeneous approach across heterogeneous cities. This homogeneity reduces the predictive power of land unavailability for house prices.

Therefore, in this paper, we construct new measurements of the percentage of undevelopable land in a geographic area where the levels of spatial aggregation span cities, counties, commuting zones, zip codes, and various polygons related to these entities. Then, noting that any individual land unavailability proxy is likely measured with error, we employ machine-learning techniques to combine land unavailability estimates computed at multiple levels of disaggregation.

First, we employ higher-resolution satellite imagery from the USGS than that used in the original Saiz dataset (see section 2). Then for each census geographic delineation, we compute multiple land unavailability proxies at several levels of disaggregation, as the optimal polygon with which to calculate land unavailability likely varies across geographies.

Figure 2 shows an example of our approach for the Los Angeles-Long Beach-Anaheim CBSA using the 2015 delineations employed in the Freddie Mac house price dataset and GMNS. In panel A, as a baseline, we draw the Los Angeles CBSA polygon (blue lines) on top of Google satellite imagery for the greater LA and surrounding areas. Compared to the 1999 MSA definition used by Saiz (figure 1), we can see that the 2015 CBSA polygon includes the southern LA cities of Anaheim and Irvine, as noted above. Differences in geographic delineations over time thus present notable challenges for researchers. Indeed, porting land unavailability across delineations may bias the relationship between land unavailability and house prices. Hence, an immediate benefit of our dataset is that we compute LU for multiple geographic definitions ranging from 1990 through 2020. Matching land unavailability to the delineations used in other datasets eliminates a vector of uncertainty for researchers studying housing markets.

Returning to figure 2, panels B to D show the polygons that our methodology exploits to

measure land unavailability. We consider various buffered polygons around the first principal city (panel B), buffers around the CBSA polygon (panel C), and circles around the principal city centroid (panel D).

In panel B, we calculate land unavailability within the first principal city polygon (by population size; orange polygon), corresponding to the Los Angeles principal city. Then, we buffer this polygon by 10 percent (inner yellow polygon) and calculate land unavailability. From there, we sequentially increase the buffer size by 10 percentage points until the buffer reaches 150 percent (outer yellow polygon) of the original principal city polygon. The result is 16 polygons around the first principal city. These polygons allow us to directly capture land unavailability at the population-weighted center of a CBSA.

We apply the same approach to the overall CBSA polygon (figure 2, panel C), yielding five additional polygons corresponding to the CBSA polygon with buffers ranging from 0 to 20 percent. The advantage of buffering the CBSA polygon is that it covers the whole CBSA and accounts for idiosyncrasies in the polygon's shape. Finally, in panel D, we expand Saiz's original approach by considering multiple circles around the first principal city centroid instead of just within a 50k km radius circle. In the case of Los Angeles in panel D, larger circles may be appropriate as they cover eastern LA, including San Bernardino and Riverside, and southern Los Angeles. Panel D shows how we exploit nine distinct circles with radii around the first principal city centroid ranging from 20k to 100k km (by 10k increments). Overall, figure 2 exemplifies how we calculate land unavailability for 30 different polygons for each CBSA. However, the best land unavailability predictor for house prices is likely a combination of individual land unavailability estimates.

Thus, the second step of our approach uses these various land unavailability (LU) proxies and machine learning (ML) techniques to predict house prices and create the LU-ML IV. Our ML framework spans housing datasets and econometric setups. Output from our approach is either (1) a cross-sectional dataset with a single land unavailability estimate for each geographic unit; or (2) a panel dataset of LU-based predictors.

Here, we describe our methodology within a panel data setup, but our framework easily

extends to long-differenced empirical specifications as well.

First, we difference house prices by, for example, using year-over-year log first differences. For each time period we then create 5 repeats of 5 folds of the data. Next, within each fold, we implement a cross-fitting approach where we train the XGBoost algorithm using a training set and predict house prices out-of-sample for the holdout (test) set. The average predictions across each repeat by CBSA and time period represent the final house price predictions and thus the LU-ML IV for house price growth.

More plainly, for each time period t in the panel dataset:

1. Randomly split the data into 5 equal chunks (5 folds).
2. Choose one chunk as the holdout (test) set, where the other chunks constitute the training set (used for training or estimating the XGBoost algorithm).
3. Train the XGBoost algorithm on the training data.
4. Predict house price growth out-of-sample for the holdout set (cross-fitting).
5. Repeat steps (2) to (4), allowing each of the other chunks (folds) to serve as the holdout set.
6. Repeat steps (1) to (5) 5 times (5 repeats).
7. Average the out-of-sample house price growth predictions across all repeats by CBSA to generate the LU-ML IV for time period t house price growth.

Repeating the above steps for each time period yields a panel dataset representing the LU-ML instrument. If the endogenous house price growth variable is in long-differenced form, generate a cross-sectional LU-ML IV by following steps (1) to (7) once.

We guard against overfitting in the construction of the LU-ML IV (as data overfitting would lead to bias in 2SLS estimates) by (1) using early stopping within the XGBoost algorithm¹⁰ and (2) cross-fitting. Early-stopping is an estimation technique commonly employed when training XGBoost algorithms, where training is stopped if the target error does not improve after a certain number of rounds relative to a validation set within each fold. Cross-fitting, an approach used in the double machine learning literature to mitigate overfitting ([Chernozhukov et al., 2018](#)), mandates that our above algorithm only uses out-of-sample

¹⁰See https://xgboost.readthedocs.io/en/stable/python/python_intro.html#early-stopping.

predictions for the holdout set as the final instrument for house price growth (e.g., step 4 above).

Using out-of-sample predictions via cross-fitting also adds an additional layer of exogeneity to the LU-ML IV as they represent the projection of a broader land unavailability–house price relationship onto each region. This ensures instrument independence from local idiosyncrasies that may contaminate the 2SLS causal chain from land unavailability through house prices to the outcome of interest. Our LU-ML IV approach thus extends a substantive literature starting with [Bartik \(1991\)](#) that projects national data onto local regions for instrument exogeneity.

Overall, the flexibility of the above algorithm makes it applicable to various house price datasets and econometrics setups, allowing us to easily create an LU-ML IV for a wide range of research problems. Moreover, by using machine-learning methods to parse a multitude of local land unavailability proxies, the LU-ML IV has strong predictive power for house prices. Below, we demonstrate the utility of our land unavailability approach in several important housing market applications.

4 LU and Housing Wealth Elasticities

Our first application uses the LU-ML IV to re-estimate the housing wealth elasticities in [Mian and Sufi \(2014\)](#) and [Guren et al. \(2021, GMNS\)](#) that originally employed Saiz elasticity as an instrument for house prices.¹¹ We document that the LU-ML IV has substantially stronger first stage predictive power than Saiz elasticity within both the long-differenced regressions of Mian and Sufi and the panel data setup in GMNS. The more accurate first stage predictions increase the precision of second stage estimates, reducing the uncertainty surrounding the impact of changes in housing wealth.

4.1 Great Recession Era Housing Net Worth and Non-Tradable Employment

Mian and Sufi examine the impact of falling housing net worth on non-tradable employment during the Great Recession via the long-differenced regression shown in equation 1. Columns

¹¹As Saiz elasticity has low predictive power, Guren et al. also develop a sensitivity instrument, as we discuss below.

1 to 4 of table 3 replicate Mian and Sufi's key OLS and IV results. Note that Mian and Sufi consider two proxies for non-tradable employment: restaurant and retail employment (*Rest.* & *Retail*) or employment in industries with low geographic concentration (*Geog. Concen.*).¹² In both Mian and Sufi's OLS and IV results, falling housing net worth reduces non-tradable employment. Yet instrumenting changes in housing net worth with Saiz elasticity leads to large 2SLS standard errors (columns 3 and 4). This statistical imprecision stems from the moderate first stage predictive power of the Saiz IV, with a first stage *F*-statistic of just 11.07 and a first stage partial R^2 (the incremental predictive power of just the instrument) of 0.12. Moreover, because of the limited geographic coverage of the Saiz IV, the number of counties drops from 944 in columns 1 and 2 (OLS) to just 540 in columns 3 and 4 (Saiz IV). This sizable drop in observations makes the OLS and IV results difficult to compare.

Columns 5 and 6 exploit the LU-ML IV but retain counties with an available Saiz elasticity estimate (those used in columns 3 and 4). Moving from Saiz elasticity to the LU-ML IV increases first stage fit markedly: The first stage partial R^2 increases by a factor of four, and the first stage *F*-statistic jumps to 214.71. These more accurate first stage predictions reduce second stage standard errors by 43 percent when non-tradable employment is proxied by restaurant and retail employment (column 5 vs. column 3) and by 34 percent for non-tradable employment measured using geographic concentration (column 6 vs. column 4). This notable rise in the precision of the 2SLS estimates corresponds to a considerable reduction in uncertainty in the relationship between changes in housing net worth and non-tradable employment during the Great Recession.

Finally, columns 7 and 8 use all counties with an available LU-ML IV. The number of observations nears Mian and Sufi's full dataset (with only Alaska and Hawaii missing) and corresponds to a 73 percent increase compared to regressions that use Saiz Elasticity. This growth in sample size leads to a further decline in 2SLS standard errors for restaurant and retail employment (column 7 vs. column 5) but nearly no change when non-tradable employment is measured using geographic concentration (column 8 vs. column 6). Moreover,

¹²See [Mian and Sufi \(2014\)](#) for definitions of these variables.

as the number of observations in columns 7 and 8 is close to Mian and Sufi's full dataset, the OLS and IV specifications become more directly comparable. Indeed, the full sample 2SLS results that employ the LU-ML IV indicate that the OLS estimates in columns 1 and 2 are biased downwards.

4.2 Long Run Housing Wealth Elasticities

Next, we consider longer-run housing wealth elasticities within the framework of GMNS (equation 2). Our aim is to compare 2SLS estimates where the excluded instrument is Saiz elasticity, the LU-ML IV, or GMNS's preferred sensitivity instrument. To build their sensitivity instrument, GMNS first regress CBSA house price growth (year-over-year log first-differences) on the house price growth of the corresponding census region, with city-specific coefficients. The sensitivity instrument for each CBSA is the estimated city-specific coefficient from this regression multiplied by the house price growth for that CBSA's census region.

We replicate GMNS's primary results in table 4. GMNS estimate equation 2 for three separate periods: 1978–2017 (panel A), 1990–2017 (panel B), and 2000–2017 (panel C). OLS output is in column 1, while columns 2 and 3 show results that use the sensitivity instrument and the Saiz elasticity IV, respectively.

The OLS results for the full sample (1978–2017) correspond to an elasticity estimate of 0.083, meaning a 10 percent increase in house prices is associated with a 0.83 percent gain in retail employment. Note that theoretically that GMNS find an elasticity estimate of 0.09. Column 2 presents GMNS's preferred estimates that use the sensitivity instrument. The coefficient in panel A for the 1978–2017 period in column 2 is 0.058 with a standard error of 0.017. Compare this to the results in column 3, panel A that use the Saiz elasticity IV.¹³ In column 3, the standard error is relatively large at 0.048. The sizable standard error emanates from the low predictive power of the Saiz IV in the first stage. Indeed, the first stage F -statistic in column 3 that uses the Saiz IV is just 19.67 versus 249.08 for the sensitivity instrument (column 2). Panels B and C likewise report estimates for the 1990–2017 and

¹³To use Saiz elasticity (a cross-sectional variable) within a panel setup, GMNS multiple the Saiz elasticity proxy for each city by national-level house prices.

2000–2017 time periods.

The bottom panel of table 4 provides various notes on each specification. The regressions in column 3 that instrument house price growth with Saiz elasticity exploit data from just 270 CBSAs, compared to 380 for the overall dataset, again highlighting the meager geographic coverage of the Saiz IV. Also, GMNS use census region \times year-quarter fixed effects in columns 1 and 2 but only year-quarter fixed effects in column 3. Employing census region \times year-quarter fixed effects when Saiz elasticity is the excluded instrument further increases the second stage standard error (see table 5, column 2).

Table 5 extends the GMNS empirical framework to specifications where we instrument house price growth with land unavailability. To compare to the GMNS results, column 1 replicates the GMNS findings that use the Saiz elasticity IV (e.g., column 3 of table 4). Column 2 of table 5 again employs the Saiz IV but uses census region \times time fixed effects instead of just time fixed effects (e.g., to match the GMNS OLS and sensitivity IV estimates in columns 1 and 2 of table 4). Including the census region \times time fixed effects reduces the coefficient estimates slightly as the standard errors increase.

In column 3, the instrument is LU within a 50k km circle around each CBSA's principal city centroid, following the Saiz method. The first difference between Saiz elasticity and LU within a 50k km circle is that LU uses 2015 CBSA definitions, in line with GMNS's Freddie Mac house price dataset, whereas Saiz uses 1999 MSA/NECMA definitions. The second difference between the two instruments is that Saiz elasticity also incorporates local land use regulations from the Wharton Residential Land Use Regulatory index. As house price growth increases local regulation through political economy mechanisms, this portion of the Saiz elasticity proxy is likely not exogenous (see Davidoff (2016) for a review). Also, local land use regulations predict house price increases (Davidoff, 2016). Thus, the first stage partial R^2 statistics are higher in columns 1 and 2, which use Saiz elasticity, versus columns 3 and 4, which use LU within a 50k km circle of each CBSA's principal city centroid. In column 3, we also retain the original Saiz dataset (just 270 CBSAs). The coefficient estimates increase in all estimation periods (panels A - C) compared to column 2, but the standard

errors also jump for the 1990–2017 and 2000–2017 time periods.

Column 4 uses all CBSAs in the GMNS dataset (except those in AK and HI), and the excluded instrument remains LU calculated within a 50k km circle around each principal city centroid. The 2SLS elasticity estimates fall compared to column 3 and, in the case of the 1990–2017 and 2000–2017 periods, they do so considerably. This result indicates that housing wealth elasticities may differ across the large CBSAs in the Saiz data versus the smaller ones included in modern housing datasets. We leave the estimation of differences in housing wealth elasticities between large and small CBSAs as an avenue for future research.

Column 5 uses the LU-ML IV for a substantial gain in first stage fit. The first stage partial R^2 in panel A jumps to 0.12, a sixfold increase relative to column 2. With this considerable rise in first stage predictive power, the second stage standard errors fall precipitously. Finally, note that GMNS produce a theoretical estimate for the housing wealth elasticity of 0.09. Thus, the coefficient estimate in column 5, panel A of 0.081 for the 1978–2017 sample is near the GMNS’s theoretical result.

In column 6 of table 5, we employ both the LU-ML and GMNS sensitivity instruments. This allows us to construct a standard overidentification test for differences in 2SLS estimates based on sensitivity versus the LU-ML IV. The overidentification p -value in column 6, panel A is 0.03, indicating that for the 1978–2017 sample that we reject the null hypothesis that the LU-ML IV (e.g., column 5) and the sensitivity IV (table 4, panel A, column 2) produce the same second stage coefficients. This is not surprising as the housing wealth elasticity estimate is 0.081 when using the LU-ML IV, close to GMNS’s theoretical estimate of 0.09, versus just 0.058 for the sensitivity instrument. Yet the overidentification p -values in panels B and C of column 6 imply that we cannot reject the null hypothesis that the LU-ML and the GMNS sensitivity IVs produce the same second stage estimates for the 1990–2017 and 2000–2017 sample periods.

5 LU and Entrepreneurship During the COVID-19 Pandemic

In a second application, we examine the impact of house price growth on entrepreneurship and self-employment during COVID-19. We build on [Adelino et al. \(2015\)](#), who conduct a

similar analysis during the 2000s housing boom. Our aim is to provide evidence as to the external validity of Adelino et al. (2015) to the COVID-19 period, determine if house price growth induced different entrepreneurship rates during the pandemic relative to the 2010s, and further demonstrate the utility of our LU-ML IV.

The COVID-19 crisis was unique as substantial economic activity shut down, but house prices increased markedly in many markets. Increases in housing wealth may have affected small firm counts via equity extraction or mortgage refinance, as available cash or lower debt-service payments may have allowed entrepreneurs to start new ventures or support existing businesses. Moreover, media narratives suggest that changing preferences and expectations toward work during the pandemic sparked entrepreneurship and small firm formation.¹⁴ Yet reverse causality likely plagues naive correlations between house price changes and entrepreneurship or self-employment: Brightening local economic growth elevates house prices while rising house prices improve local economic conditions. Thus, we employ the LU-ML IV as an instrument for house prices.

More specifically, we estimate the following regression using a county-level, panel dataset:

$$\Delta NumFirms_{i,j,s,t} = \psi_i + \eta_j + \xi_{s,t} + \beta_{1,j} \mathbf{1}_j \Delta p_{i,s,t} + \beta_{2,j} \mathbf{1}_{covid} \Delta p_{i,s,t} + \Gamma X_{i,s,t} + \varepsilon_{i,j,s,t} \quad (3)$$

$\Delta NumFirms_{i,j,s,t}$ is the year-over-year log difference in the number of firms in county i , firm size category j , and state s at time t . $\Delta p_{i,s,t}$, the endogenous variable, represents the year-over-year log difference in Zillow house prices for county i in state s at time t , $\mathbf{1}_j$ is an indicator equal to 1 for firm size category j , and $\mathbf{1}_{covid}$ is an indicator equal to 1 for the COVID-19 period (2020Q2 - 2022Q2). $\beta_{1,j}$, the elasticity of firm formation to housing wealth for firm size category j , measures the percentage change in the number of firms in size category j for a 1 percent increase in house prices before COVID-19 (2011Q1 - 2020Q1). $\beta_{2,j}$ represents the change in this elasticity for firm size category j during COVID-19, relative to the pre-COVID-19 period.

House prices are from Zillow and include 1,092 counties over our sample period. As

¹⁴See “How Covid Inspired a New Generation of Entrepreneurs.” *Bloomberg News*. June 1, 2021. “Start-Up Boom in the Pandemic Is Growing Stronger.” *New York Times* August 19, 2021. “Over 5 Million New US Startups Show Covid-Era Boom Has Legs.” *Bloomberg News*. January 17, 2023.

the LU data provide complete coverage of the contiguous U.S., our cross-sectional sample is substantially larger than other studies that employ Saiz elasticity. Firm counts and size categories are from the BLS QCEW.¹⁵ We group firms into four categories based on the number of employees: $\{< 5 \text{ employees}, [5, 9], [10, 19], > 19\}$.

Based on prior research, we hypothesize that house price growth leads to increased entrepreneurship or self-employment and the formation of small firms (those with less than 5 employees) but has little effect on larger firms (e.g., those with more than 19 employees). We further aim to assess the effects of house price growth on firm formation during the pandemic, relative to the pre-pandemic period, to determine whether house price growth had an abnormally large impact on entrepreneurship and self-employment during COVID-19.

The panel data setup also allows us to include several controls and circumvent the criticisms in Davidoff (2016) regarding the use of land availability as an IV. More precisely, as the dependent variable is in year-over-year log first differences, the county fixed effects (ψ_i) capture differential long-run trends across counties over the sample period. Thus, as discussed in more detail in section 7, these county fixed effects account for Davidoff's main concern that land unavailability correlates with the long-run, city-level drivers of housing demand. Even so, as documented below, using our LU dataset with complete coverage of the contiguous U.S., we find that LU is largely uncorrelated with housing demand factors.

$\xi_{s,t}$ represents state by time fixed effects and accounts for time-varying statewide shocks, such as changes in state-level COVID-19 restrictions or evolving state-specific economic trends. Controlling for changing state-level shocks ensures that turbulent and heterogeneous statewide COVID-19 responses are not driving our results. The LU-ML IV facilitates including these granular fixed effects through its comprehensive geographic coverage and strong predictive accuracy that yields precise second stage estimates even after incorporating such controls. In contrast, using a weaker instrument or one with a limited geographic scope, such as Saiz elasticity, within equation 3 would produce imprecise 2SLS estimates.

¹⁵The BLS QCEW reports the number of firms by industry (two-digit NAICS) and size at the state level. To generate the number of firms at the county level, we apply state-level industry by size shares to the county data.

$X_{i,s,t}$ corresponds to a vector of 2010 two-digit NAICS industry shares, computed at the county level and multiplied by time fixed effects, allowing their impact to vary over time. These controls are critical as COVID-19-induced partial economic lockdowns had notably uneven effects across different industries during our sample period. Finally, η_j are firm size category fixed effects, and standard errors are clustered by county and time.

As previously noted, a key advantage of our LU-ML IV is its predictive power for house prices. Indeed, in a specification where house price growth is the dependent variable, [Adelino et al. \(2015\)](#) find a t -statistic on Saiz elasticity of 4.5 (their table 2, column 1). In comparison, in a similar regression for our time period using the controls in equation 3, the t -statistic on the LU-ML IV is 8.54. This substantial jump in the predictive accuracy of the LU-ML IV, relative to Saiz elasticity, increases the precision of second stage estimates within a 2SLS framework.

Figure 3 reports estimates from equation 3. For the pre-COVID-19 period (panel A), the OLS estimates (red) indicate that changes in housing wealth do not have a statistically significant impact on firm counts across firm size bins. Conversely, the IV estimates show that rising house prices increased counts for small firms (those with less than 5 employees) but had little effect on counts for larger firms. Specifically, IV estimates imply that a 1 percent rise in house prices led to a 0.15 percent increase in the number of small firms. These results are congruent with previous research and also suggest that the OLS estimates for the smallest firm size bin are biased downward.

Panel B plots the difference in the elasticity estimates during COVID-19 relative to the pre-COVID-19 period. For both the OLS and IV estimates, house price growth led to higher firm counts during COVID-19 for firms with less than 5 employees. The IV estimate is sizable and economically meaningful at 0.42, indicating that the elasticity of small firm counts to housing wealth nearly tripled during COVID-19 relative to pre-pandemic estimates. This result suggests that house price growth-induced entrepreneurship was stronger during the pandemic, in line with media narratives suggesting that COVID-19 changed households' preferences toward work, entrepreneurship, and self-employment.

As previously indicated, the channel underpinning our findings likely relates to households using loans backed by housing collateral or freed up capital from refinance-induced lower debt-service payments to start new businesses or buttress existing firms. We leave untangling the relevant channels for future research.

6 Buildable Land and Supply-Side Speculation

[Nathanson and Zwick \(2018\)](#) develop a theoretical model that documents how disagreement and supply-side speculation in housing markets can produce house price booms in traditionally supply elastic areas. Specifically, the model posits that homebuilders may view housing markets with intermediate amounts of land available for development (buildable land) as supply elastic in the short run but inelastic in the long run. When these homebuilders are optimistic about future prices (e.g., during a national housing boom), they acquire and subsequently bid up the prices of available land. Since land is a critical factor in housing production, this raises house prices in markets with intermediate amounts of buildable land, even in the face of large-scale construction. As a result, house prices boom in traditionally supply elastic housing markets. The supply-side speculation theory thus aims to explain the immense 2000s house price growth in areas like Phoenix, Las Vegas, Florida, and inland California.¹⁶

Nathanson and Zwick provide several pieces of evidence in support of their theory. For example, they cite a 2000s-era Pulte Homes investor presentation that stated that the traditionally elastic markets of West Palm Beach, Orlando, Tampa, Ft. Myers, Sarasota, Las Vegas, and Chicago were surprisingly constrained. A more formal test of the supply-side speculation theory would require precise data on the amount of buildable land within housing markets. To our knowledge, no such dataset previously existed.

Therefore, this section exploits detailed satellite land cover and slope image files to construct a new dataset that precisely measures the amount of buildable land across the contiguous United States.

¹⁶Note that an extensive literature studies the causes of the 2000's housing crisis and Great Recession. For an overview, see [Foote et al. \(2021\)](#) and [Griffin et al. \(2021\)](#). Here, we use this application to further demonstrate the utility of our data.

The basis of our computation is the 2001 USGS LandSat Land Cover Dataset. The LandSat Land Cover data classify land use in the United States at a spatial resolution of 30 meters. Figure 4 plots the LandSat Land Cover data for Florida. In the satellite image, red pixels correspond to developed land, where darker red pixels represent more dense development. Similarly, blue areas represent water and wetlands. The most developed area is downtown Miami (dark red in southeast Florida), and the map clearly shows how water and wetlands restrict housing expansion in that market. Oppositely, other coastal and central Florida areas are comparatively at the intermediate stages of development. They have lower density and surrounding areas that appear available for construction.

We compute the land area available for development within each housing market by first removing developed land (e.g., red pixels on the Florida map) as well as water and wetlands (blue pixels). We also remove steep sloped terrain measured using USGS 1 arc-second DEM slope files (using no buffer for polygons in the shapefiles) and exclude regions designated as parks using a shapefile from data.gov. We then calculate the land area of the remaining buildable land. In a sense, buildable land is the complement to land unavailability but additionally classifies start of period developed land (2001) and parks as unavailable as well.

Three-digit zip codes serve as the unit of aggregation for our buildable land calculation. The U.S. Postal Service developed zip codes in the 1960s with similar populations across delineations. Hence, they better reflect pre-2000s housing boom U.S. populations and geographies, especially in the Western U.S. In contrast, counties or CBSAs vary drastically in size and stem from area definitions dating back to the 1800s.¹⁷

To test the relationship between buildable land and 2002–06 house price growth, we group three-digit zip codes into 2001 buildable land deciles. Summary statistics are in table 6. Column 1 shows the buildable land decile, and column 2 displays the average amount of buildable land for three-digit zip codes in that buildable land decile (thousands of square kilometers). As expected, in column 2, buildable land monotonically increases over buildable land deciles. Column 3 shows the mean percentage of buildable land (relative to all available

¹⁷For example, the land area of the Riverside-San Bernardino CBSA is 260 percent larger than the land area of the entire state of Massachusetts.

land) within each buildable land decile. Notice that there is minimal available buildable land in deciles 1 and 2. Three-digit zip codes in these deciles are the “inelastic” housing markets characterized by Nathanson and Zwick that likely have both high land unavailability and regulatory supply restrictions.¹⁸ For other buildable land deciles, the percentage of buildable land is monotonically increasing. A potential concern when using buildable land defined within three-digit zip codes, which can vary in size, is that buildable land may be a function of available land. We partially address this concern in column 4 and show the correlation between available and buildable land by buildable land decile. The correlations are wide-ranging, and only in buildable land decile 10 is the correlation with available land over 0.5. We return to this issue below.

Figure 5 maps three-digit zip codes by buildable land decile. Red areas signify buildable land decile 1 (least amount of buildable land), blue areas represent buildable land decile 5 (intermediate amount of buildable land), and yellow areas map buildable land decile 10 (largest amount of buildable land). Buildable land decile 1 corresponds to housing markets traditionally considered inelastic due to density, land unavailability, and regulatory constraints. These housing markets include New York City, Boston, Miami, downtown Tampa, New Orleans, downtown Chicago, downtown Milwaukee, coastal Los Angeles, and areas adjacent to the San Francisco Bay. Three-digit zip codes in buildable land decile 5 (intermediate amounts of buildable land, blue) consist of suburban areas in inland southern California, central California, and northern California. Buildable land decile 5 also includes Las Vegas, Phoenix, Colorado Springs, suburban regions in central and coastal Florida, suburban Chicago, and several suburban housing markets in the northeast. Finally, yellow areas showing buildable land decile 10 are mainly rural regions in the Midwest and Texas.

Note that Nathanson and Zwick’s supply-side speculation theory aims to explain housing markets with *intermediate* land supply. They hence concede that supply inelastic markets should also experience sizable house price growth during a boom (e.g., [Saiz \(2010\)](#)) and that the house price growth in inelastic markets is not the focus of their theory. Thus, the null

¹⁸See also the references in [Nathanson and Zwick \(2018\)](#).

hypothesis of interest is that house price growth in traditionally supply elastic areas with intermediate quantities of buildable land equals house price growth in areas with relatively smaller or relatively larger amounts of buildable land. A rejection of this null supports the supply-side speculation theory and would yield a hump-shaped, non-monotonic relationship between buildable land deciles and house price growth.

We evaluate the supply-side speculation theory in table 7 by regressing 2002–06 three-digit zip code house price growth on 2001 buildable land decile indicator variables. Robust standard errors are clustered at the state level. Column 1 shows the mean house price growth within each buildable land decile. Not surprisingly, house price growth is highest in areas with the least buildable land (buildable land decile 1 corresponding to inelastic markets), at 58.6 percent. Yet the second highest mean house price growth is in buildable land decile 5 at 44.1 percent, followed closely by buildable land decile 4 at 42.9 percent. House price growth in buildable land deciles 2 and 3 is substantially smaller at 35 and 27 percent, respectively.¹⁹ Similarly, house price growth is markedly lower for buildable land deciles 6 through 10. Note also that the R^2 of the regression is 25 percent, and thus 2001 buildable land deciles explain a large portion of the cross-sectional variation in house price growth during the 2000s. Together, this evidence suggests that inelastic areas and housing markets with intermediate amounts of buildable land experienced the largest house price growth during the 2000s boom.

Columns 2 and 3 statistically test the supply-side speculation theory. Here we exclude the indicator for buildable land decile 5 but retain the intercept. Thus, the intercept is house price growth for buildable land decile 5, and the regression coefficients are the difference in mean house price growth relative to decile 5. The coefficients on the indicators for buildable land deciles 2, 3, and 6 - 10 are all negative and statistically significant in column 2. Hence, three-digit zip codes in buildable land deciles 2, 3, and 6 - 10 experienced noticeably lower house price growth than three-digit zip codes with intermediate amounts of buildable land. Similarly, column 3 shows that controlling for Bartik labor demand shocks does not affect our

¹⁹Buildable land decile 2 also likely contains inelastic housing markets, perhaps accounting for its slightly higher house price growth relative to decile 3.

results.²⁰ Together, these regressions document that three-digit zip codes with intermediate amounts of buildable land experienced statistically larger house price growth from 2002–06, congruent with the supply-side speculation theory.

As noted above, a potential concern in constructing buildable land within three-digit zip codes is that buildable land may be a function of available land. Hence, the amount of available land within a three-digit zip code may be driving our results. We address this concern with a falsification test. More precisely, we retain all three-digit zip codes outside of buildable land deciles 1 (inelastic areas) and 5 (intermediate buildable land areas). Of these remaining regions, we then collect the three-digit zip codes whose available land is within the range of available land for the original buildable land decile 5. This yields 294 (out of 607) three-digit zip codes. The mean house price growth for these regions is 25.1 percent. All other three-digit zip codes outside of our original buildable land deciles 1 and 5 have a mean house price growth of 31.9 percent. The difference of -6.8 percentage points is statistically significant at the 1 percent level (robust t -stat = -2.6). Therefore, other three-digit zip codes whose available land is within the range of the available land for regions in buildable land decile 5 have *lower* house price growth. The results from this falsification test thus suggest that buildable land, and not available land, drive the above relationship between buildable land and house price growth.

7 Correlations Between LU and Housing Demand Proxies

The use of land unavailability as an instrument relies on its exogeneity, meaning that it should not be positively correlated with the unobserved determinants of housing demand. In the literature, there is debate on this issue. [Mian and Sufi \(2011, 2014\)](#) claim that land unavailability is exogenous, while [Davidoff \(2016\)](#) contends that land unavailability is positively correlated with housing demand factors. Davidoff's critique posits that regions with high land unavailability also have experienced positive correlation with other key house price drivers such as education, immigration, and the economics of agglomeration. Davidoff

²⁰The Bartik is demeaned relative to the entire sample so that the intercept can be interpreted as the mean house price growth in decile 5 in a three-digit zip code with an average Bartik shock.

further suggests that the impact of these variables has been increasing over time and therefore cannot be differenced out in a long-differenced regression.

Before exploring correlations between land unavailability and housing demand factors, we first note that the exogeneity of any instrument, including land unavailability, depends on the econometric specification, the dependent and endogenous variables, and the time period under study. Thus, researchers should independently assess their instrument's validity, realizing that certain empirical designs are more likely to lend credence to instrument exogeneity. For example, in the panel data specifications of equations 2 and 3, both the dependent and endogenous variables are differenced. The included city- or county-level fixed effects thus control for differential long-run trends across cities and Davidoff's main concern surrounding the exogeneity of the land availability.

Returning to correlations between land unavailability and housing demand factors, we first highlight that our study differs from other attempts to examine the exogeneity of land unavailability as we use a more highly disaggregated dataset with complete coverage of the contiguous U.S. In contrast, previous assessments employed the limited numbers of MSAs available in the Saiz data and thus suffer from a sample selection issue. MSAs only cover a fraction of U.S. land area. This limited coverage biases any correlations between land unavailability and housing demand factors towards regions with higher levels of historical development (e.g., the northeastern U.S.). Indeed, for a city to be classified as an MSA using the 1999 Saiz delineations, it must have a population of at least 50,000. As land unavailability increases the cost of construction, MSAs are less likely to be located in areas with high land unavailability, all else equal.

To see this, consider figure 6, which plots Google satellite imagery for the U.S. and coverage for Saiz elasticity. As in the Saiz dataset, the red circles have a 50k km radius around each MSA's first central city centroid. The figure clearly shows a strong negative correlation between the instances of MSAs and land unavailability due to rugged terrain, for example. This pattern surfaces in the Rocky Mountain region, where five MSAs sit at the base of the Rockies in Colorado. Yet even in the populated pacific states (California,

Washington, and Oregon), there is a negative relationship between MSA instantiation and terrain slope. Indeed, the northern ascent of California MSAs is limited by the Mendicino and Shasta National Forests, while Seattle lies between Olympic National Park and Wenatchee National Forest. Thus, judging the exogeneity of land unavailability using only MSAs will lead to biased results.

Table 8 lists correlations between housing demand proxies and our land unavailability estimates with near complete coverage of the U.S. Specifically, we compile various determinants of housing demand at the zip code level and run separate regressions of each housing demand factor on zip code, three-digit zip code, and county land unavailability.²¹ Each cell in table 8 thus represents the output from a different regression. We measure land unavailability within a five percent buffer around each geographic polygon. The table shows the regression coefficients with standard errors clustered at the two-digit zip code level in parentheses.

Findings indicate that land unavailability measured at the zip code, three-digit zip code, or county levels is uncorrelated with log household income in 2001, 2019, and the difference in household income between 2001 and 2019. Land unavailability measured at the three-digit zip code or county level also has no correlation with business payrolls (2000, 2019, and difference), employment (2000, 2019, and difference), the number of households (2001, 2019, and difference), the log change in the number of business establishments between 2000 and 2019, the college share in 2000, the foreign share in 2000, and an amenities index. The lack of correlation between land unavailability, for three-digit zip codes or counties, and these housing demand factors supports using land unavailability as an instrument for house prices.

Measured at the zip code level, land unavailability is negatively correlated with business payrolls, employment, and the number of households in 2000–01 and 2019. These negative correlations are unsurprising as high land unavailability impairs residential and commercial construction. Indeed, given their small geographic size, the impacts of high land unavailabil-

²¹IRS household income and the number of households is from the IRS Statistics of Income; business payrolls, employment, and business establishments are from the Census County Business Patterns; the college and foreign shares are from the 2000 census; and the amenities index is from a large internet aggregator of such data.

ity are often more acute for zip codes than for three-digit zip codes or counties where pockets of severe land unavailability can be averaged out over a larger area. Thus, negative correlations can ensue at the zip code level in table 8, even when there is no statistical association at wider geographic aggregations. Note also that only positive correlations are a concern for the exogeneity of land unavailability, as positive associations suggest that land unavailability is a conduit for higher productivity. This implies that the negative correlations between zip code land unavailability and these housing demand variables are not a threat to the validity of land unavailability as an instrument for house prices.

Furthermore, table 8 shows that land unavailability at the zip code level is uncorrelated with the two-decade-long changes in business payrolls, employment, and the number of households. Thus, the relationship between these variables and land unavailability is fixed, contrary to the concerns of Davidoff (2016) that the drivers of housing demand have become more acute over time in high land unavailability areas. Indeed, such static differences can easily be differenced out in a long-differenced regression or accounted for using fixed effects. Finally, the bottom panel of table 8 shows that land unavailability measured at the zip code level is uncorrelated with the change in business establishments between 2000 and 2019 and the college share in 2000, while being negatively correlated with the foreign share in 2000 and an amenities index. As noted above, these latter negative correlations are not surprising for land unavailability measured at the zip code level.

Another key determinant of housing demand is changes to labor demand within a city. We follow Davidoff (2016) and employ Bartik (1991) labor demand shocks at the county level. We assess the correlation between LU and labor demand shocks through the following specification, estimated separately for each year from 2001 to 2019:

$$Bartik_i = \alpha + \beta \cdot LU_i + \epsilon_i \quad (4)$$

$Bartik_i$ represents the annual BLS QCEW Bartik shock for county i , and LU is land unavailability for county i computed using a 5 percent buffer around each county polygon. The results are in figure 7, where error bars correspond to ± 2 robust standard errors clustered at the state level. The figure shows that Bartik labor demand shocks are largely uncorrelated

with LU since 2000.

Overall, the findings in this section indicate that LU is uncorrelated with key housing demand factors. These results broadly support using land unavailability as an instrument for house prices.

8 Conclusion

This paper combines high-resolution satellite imagery with machine-learning techniques to provide new estimates of the geographic determinants of U.S. housing supply. Our land unavailability-machine learning instrument (the LU-ML IV) is a markedly more accurate house price predictor than Saiz elasticity.

In several applications, we highlight the utility of our land unavailability data. First, in the canonical problem of estimating housing wealth elasticities, we show that using the LU-ML IV increases first stage predictive power substantially compared to Saiz elasticity. As such, the precision of the second stage estimates rises precipitously, reducing uncertainty in housing wealth elasticity estimates. We also provide new evidence on the causal impact of house price growth on entrepreneurship and self-employment during the COVID-19 pandemic. In a 2SLS research design using the LU-ML IV as an instrument for house prices, estimates show that house price growth increased small firm counts but had little impact on the number of larger firms. Moreover, congruent with media narratives indicating that the pandemic changed households' preferences toward work, we find that the housing wealth-induced entrepreneurship rate was much higher during the pandemic than in the 2010s. Third, we build a new dataset that measures the available buildable land within a geographic polygon. Buildable land is the amount of available land less previous development, parks, and the components of land unavailability (steeped sloped terrain, water, and wetlands). Using buildable land, we perform new statistical tests for the supply-side speculation theory ([Nathanson and Zwick, 2018](#)). Finally, we find that land unavailability is broadly uncorrelated with housing demand factors, supporting its use as an instrument for house prices.

As real estate continues to play a leading role in household and broader economic activity,

researchers will likely find our land unavailability and buildable land datasets useful as house price instruments, predictors, control variables, or geographic proxies for supply constraints across regions.

References

- M. Adelino, A. Schoar, and F. Severino. House prices, collateral, and self-employment. *Journal of Financial Economics*, 117(2):288–306, 2015.
- A. Aladangady. Housing wealth and consumption: Evidence from geographically-linked microdata. *American Economic Review*, 107(11):3415–46, November 2017.
- T. J. Bartik. *Who Benefits from State and Local Economic Development Policies?* Books from Upjohn Press. W.E. Upjohn Institute for Employment Research, November 1991.
- N. Baum-Snow and L. Han. The microgeography of housing supply. *Working Paper*, 2020.
- S. Büchler, M. v. Ehrlich, and O. Schöni. The amplifying effect of capitalization rates on housing supply. *Journal of urban economics*, 126:103370, 2021.
- T. Chaney, D. Sraer, and D. Thesmar. The collateral channel: How real estate shocks affect corporate investment. *The American Economic Review*, 102(6):2381–2409, 2012.
- V. Chernozhukov, D. Chetverikov, M. Demirer, E. Duflo, C. Hansen, W. Newey, and J. Robins. Double/debiased machine learning for treatment and structural parameters. *The Econometrics Journal*, 21(1):C1–C68, 01 2018. ISSN 1368-4221.
- J. N. Conklin, W. S. Frame, K. Gerardi, and H. Liu. Villains or scapegoats? the role of subprime borrowers in driving the us housing boom. *Journal of Financial Intermediation*, page 100906, 2021.
- T. Davidoff. Supply constraints are not valid instrumental variables for home prices because they are correlated with many demand factors. *Critical Finance Review*, 5(2):177–206, 2016.
- J. V. Duca, J. Muellbauer, and A. Murphy. What drives house price cycles? International experience and policy issues. *Journal of Economic Literature*, 59(3):773–864, 2021.
- C. L. Foote, L. Loewenstein, and P. S. Willen. Cross-sectional patterns of mortgage debt during the housing boom: evidence and implications. *The Review of Economic Studies*, 88(1):229–259, 2021.
- S. Gabriel, M. Iacoviello, and C. Lutz. A crisis of missed opportunities? Foreclosure costs and mortgage modification during the great recession. *The Review of Financial Studies*, 34(2):864–906, 2021.
- W. Gamber, J. Graham, and A. Yadav. Stuck at home: Housing demand during the covid-19 pandemic. *Working Paper*, 2021.
- J. M. Griffin, S. Kruger, and G. Maturana. What drove the 2003–2006 house price boom and subsequent collapse? disentangling competing explanations. *Journal of Financial Economics*, 141(3):1007–1035, 2021.
- A. Gupta, V. Mittal, J. Peeters, and S. Van Nieuwerburgh. Flattening the curve: Pandemic-induced revaluation of urban real estate. *Journal of Financial Economics*, 2021. ISSN 0304-405X.

- A. M. Guren, A. McKay, E. Nakamura, and J. Steinsson. Housing wealth effects: The long view. *The Review of Economic Studies*, 88(2):669–707, 2021.
- A. Mian and A. Sufi. The consequences of mortgage credit expansion: Evidence from the us mortgage default crisis. *The Quarterly Journal of Economics*, 124(4):1449–1496, 2009.
- A. Mian and A. Sufi. House prices, home equity-based borrowing, and the US household leverage crisis. *The American Economic Review*, 101(5):2132–2156, 2011.
- A. Mian and A. Sufi. What explains the 2007–2009 drop in employment? *Econometrica*, 82(6):2197–2223, 2014.
- A. Mian, K. Rao, and A. Sufi. Household balance sheets, consumption, and the economic slump. *The Quarterly Journal of Economics*, 128(4):1687–1726, 2013.
- C. G. Nathanson and E. Zwick. Arrested development: Theory and evidence of supply-side speculation in the housing market. *The Journal of Finance*, 73(6):2587–2633, 2018.
- A. Saiz. The geographic determinants of housing supply. *The Quarterly Journal of Economics*, 125(3):1253–1296, 2010.
- Y. Tan, Z. Wang, and Q. Zhang. Land-use regulation and the intensive margin of housing supply. *Journal of Urban Economics*, 115:103199, 2020.

A Tables and Figures

Table 1: Non-Tradable Employment and the Housing Net Worth Shock

	<i>Non-Tradable Emp. Growth, 2007-09</i>			
	Rest. & Retail	Geog. Concen.	Rest. & Retail	Geog. Concen.
	(1)	(2)	(3)	(4)
Δ Housing Net Worth, 2006-09	0.374*** (0.132)	0.208** (0.086)	0.201*** (0.061)	0.219*** (0.058)
First Stage <i>F</i> -Stat	11.07	11.07	182.33	182.33
First Stage Partial R^2	0.12	0.12	0.48	0.48
Instrument	Saiz Elasticity	Saiz Elasticity	LU-ML IV	LU-ML IV
Number of Counties	540	540	936	936

Notes: Columns 1 and 2 replicate Mian and Sufi (2014). Mian and Sufi proxy non-tradable employment via the restaurant and retail sector (*Rest. and Retail*) or through industries that have low geographic concentration (*Geog. Concen.*). The instrument used in columns 3 and 4 employs the XGBoost machine learning algorithm to combine Land Unavailability estimates measured at multiple levels of disaggregation to generate an out-of-sample prediction of housing net worth that is then used as the excluded instrument. Controls include 23 two-digit 2006 employment shares. Robust standard errors are clustered by state. One, two, or three asterisks represent statistical significance at the 10, 5, and 1 percent levels, respectively.

Table 2: 2SLS Housing Wealth Elasticity Estimates – 1978–2017

<i>Dependent variable:</i>		
	(1)	(2)
YoY Log Diff in Retail Emp Per Capita		
YoY Log Diff in House Prices	0.082 (0.054)	0.081*** (0.019)
First Stage <i>F</i> -Stat	14.37	187.70
First Stage Partial <i>R</i> ²	0.02	0.12
Instrument	Saiz Elasticity	LU-ML IV
Num. CBSAs	270	376

Notes: Column 1 replicates Guren et al. (2021) but uses time \times census region fixed effects instead of the time fixed effects used in Guren et al. The instrument in column 2 uses the XGBoost machine learning algorithm to combine Land Unavailability estimates measured at multiple levels of disaggregation to generate an out-of-sample prediction of house prices that is then used as the excluded instrument. Controls include CBSA fixed effects, census region \times time fixed effects, industry shares \times time, and the prediction controls in Guren et al. Robust standard errors are clustered by CBSA and time. One, two, or three asterisks represent statistical significance at the 10, 5, and 1 percent levels, respectively.

Table 3: Non-Tradable Employment and the Housing Net Worth Shock

		Non-Tradable Emp. Growth, 2007-09							
		Rest. & Retail	Geog. Concen.	Rest. & Retail	Geog. Concen.	Rest. & Retail	Geog. Concen.	Rest. & Retail	Geog. Concen.
	(1)	(2)	(3)	(4)	(5)	(6)	(7)	(7)	(8)
Δ Housing Net Worth, 2006-09	0.174*** (0.022)	0.166*** (0.017)	0.374*** (0.132)	0.208** (0.086)	0.225*** (0.075)	0.192*** (0.057)	0.201*** (0.061)	0.219*** (0.058)	
First Stage F-Stat		11.07	11.07	214.71	214.71	182.33	182.33		
First Stage Partial R^2		0.12	0.12	0.48	0.48	0.48	0.48	0.48	
Specification	OLS	IV	IV	IV	IV	IV	IV	IV	
Instrument		Saiz	Saiz	LU-ML	LU-ML	LU-ML	LU-ML	LU-ML	
Number of Counties	944	944	540	540	540	540	540	936	936

Notes: Columns 1 to 4 replicate Mian and Sufi (2014). Mian and Sufi proxy non-tradable employment via the restaurant and retail sector (*Rest. and Retail*) or through industries that have low geographic concentration (*Geog. Concen.*). Columns 3 - 6 use the LU-ML IV. This instrument employs the XGBoost machine learning algorithm to combine Land Unavailability estimates measured at multiple levels of disaggregation to generate an out-of-sample prediction of housing net worth that is then used as the excluded instrument. The counties used in columns 4 and 5 match those with available Saiz elasticity estimates (columns 3 and 4). Controls include 23 two-digit 2006 employment shares. Robust standard errors are clustered by state. One, two, or three asterisks represent statistical significance at the 10, 5, and 1 percent levels, respectively.

Table 4: Replication of Guren et al. (2021), Table 1

<i>Dependent variable:</i>			
YoY Log Diff in Retail Emp Per Capita			
	(1)	(2)	(3)
Panel A: 1978–2017			
YoY Log Diff in HP Growth	0.083*** (0.007)	0.058*** (0.017)	0.084* (0.048)
First Stage <i>F</i> -Stat		249.08	19.67
First Stage Partial <i>R</i> ²		0.16	0.03
Observations	59,999	59,999	42,710
Panel B: 1990–2017			
YoY Log Diff in HP Growth	0.081*** (0.008)	0.072*** (0.015)	0.141*** (0.037)
First Stage <i>F</i> -Stat		440.81	20.41
First Stage Partial <i>R</i> ²		0.27	0.04
Observations	41,985	41,985	29,867
Panel C: 2000–2017			
YoY Log Diff in HP Growth	0.068*** (0.008)	0.055*** (0.014)	0.134*** (0.035)
First Stage <i>F</i> -Stat		351.11	21.12
First Stage Partial <i>R</i> ²		0.31	0.05
Observations	26,884	26,884	19,116
Specification	OLS	IV	IV
Instrument		Sensitivity	Saiz Elast
Num. CBSAs	380	380	270
Yr-Qtr FE			✓
Region, Yr-Qtr FE	✓	✓	
CBSA FE	✓	✓	✓

Notes: Replication of [Guren et al. \(2021\)](#), table 1. One, two, or three asterisks represent statistical significance at the 10, 5, and 1 percent levels, respectively.

Table 5: 2SLS Housing Wealth Elasticity Estimates Using Saiz Elasticity and Land Unavailability

	Dependent variable: YoY Log Diff in Retail Emp Per Capita					
	(1)	(2)	(3)	(4)	(5)	(6)
Panel A: 1978–2017						
YoY Log Diff in House Prices	0.084* (0.048)	0.082 (0.054)	0.143*** (0.053)	0.136*** (0.057)	0.081*** (0.019)	0.066*** (0.014)
First Stage Partial R^2	0.03	0.02	0.01	0.01	0.12	0.23
OverID p-value					0.03	
Panel B: 1990–2017						
YoY Log Diff in House Prices	0.141*** (0.037)	0.136*** (0.040)	0.166*** (0.058)	0.084 (0.063)	0.083*** (0.018)	0.075*** (0.014)
First Stage Partial R^2	0.04	0.04	0.02	0.01	0.15	0.34
OverID p-value					0.28	
Panel C: 2000–2017						
YoY Log Diff in House Prices	0.134*** (0.035)	0.121*** (0.037)	0.145** (0.058)	0.050 (0.066)	0.074*** (0.021)	0.059*** (0.013)
First Stage Partial R^2	0.05	0.05	0.02	0.02	0.15	0.36
OverID p-value					0.06	
Instrument(s)	Saiz Elasticity	Saiz Elasticity	LU 50km Circles	LU 50km Circles	LU-ML, Circles	LU-ML, Sensitivity
Num. CBSAs	270	270	270	376	376	376
Date FE	✓		✓	✓	✓	✓
Region × Date FE						✓

*p<0.1; **p<0.05; ***p<0.01

Note:

Table 6: Buildable Land (BL) Summary Statistics by Decile

BL Decile (1)	BL Mean (km ² , 000s) (2)	BL Percent (3)	Corr with Available Land (4)
1	12.18	0.07	0.46
2	113.06	0.20	0.34
3	355.81	0.33	0.34
4	1013.92	0.41	0.34
5	2058.12	0.48	0.27
6	3516.77	0.58	0.46
7	5084.49	0.61	0.15
8	6883.83	0.67	0.26
9	9535.30	0.71	0.48
10	20188.21	0.75	0.83

Notes: Summary Statistics for buildable land (BL) deciles based on three-digit zip codes.

Table 7: 2002–06 House Price Growth by Buildable Land Decile

Dependent variable:			
	$\Delta(\ln HP)_{2002-06}$		
	(1)	(2)	(3)
Buildable Land Decile 1	58.597*** (4.887)	14.518*** (4.611)	13.283** (5.322)
Buildable Land Decile 2	35.124*** (4.717)	-8.955*** (3.276)	-9.166*** (3.484)
Buildable Land Decile 3	27.319*** (3.164)	-16.760*** (4.628)	-18.068*** (4.419)
Buildable Land Decile 4	42.914*** (3.664)	-1.165 (2.918)	-1.819 (3.166)
Buildable Land Decile 5	44.079*** (4.833)		
Buildable Land Decile 6	29.078*** (3.060)	-15.001*** (3.781)	-13.624*** (3.755)
Buildable Land Decile 7	21.289*** (2.356)	-22.790*** (3.971)	-20.849*** (3.906)
Buildable Land Decile 8	23.240*** (3.066)	-20.839*** (3.798)	-20.751*** (3.742)
Buildable Land Decile 9	24.520*** (3.819)	-19.559*** (4.662)	-19.910*** (4.667)
Buildable Land Decile 10	25.174*** (4.171)	-18.905*** (5.802)	-22.593*** (5.862)
Bartik Labor Demand Shock ₂₀₀₂₋₀₆			2.074*** (0.637)
Constant		44.079*** (4.833)	44.481*** (4.631)
Observations	757	757	757
R ²	0.250	0.250	0.280

Notes: 2002–06 house price growth means by buildable land decile. In column 1, the intercept is excluded, and each coefficient represents the mean house price growth for the given buildable land decile. The excluded dummy in columns 2 and 3 is buildable land decile 5, and thus coefficients represent the difference in means relative to decile 5. Robust standard errors are clustered at the state level.

Table 8: Correlations Between Land Unavailability and Housing Demand Factors

LHS Variable	Zip LU (1)	Zip3 LU (2)	Cnty LU (3)
log(IRS Household Income) ₂₀₀₁	0.0003 (0.0006)	0.0006 (0.0007)	0.0013 (0.0007)
log(IRS Household Income) ₂₀₁₉	0.0007 (0.0006)	0.0006 (0.0008)	0.0013 (0.0007)
$\Delta \log(\text{IRS Household Income})_{2019-2001}$	0.0004 (0.0003)	-0.0000 (0.0004)	0.0000 (0.0003)
log(Business Payrolls) ₂₀₀₀	-0.0158* (0.0032)	-0.0010 (0.0051)	0.0057 (0.0044)
log(Business Payrolls) ₂₀₁₉	-0.0165* (0.0032)	-0.0006 (0.0052)	0.0050 (0.0046)
$\Delta \log(\text{Business Payrolls})_{2019-2000}$	-0.0007 (0.0006)	0.0004 (0.0008)	-0.0007 (0.0007)
log(Employment) ₂₀₀₀	-0.0144* (0.0028)	-0.0010 (0.0045)	0.0048 (0.0039)
log(Employment) ₂₀₁₉	-0.0151* (0.0030)	-0.0004 (0.0048)	0.0047 (0.0043)
$\Delta \log(\text{Employment})_{2019-2000}$	-0.0007 (0.0005)	0.0006 (0.0007)	-0.0002 (0.0006)
log(Num. Households) ₂₀₀₁	-0.0095* (0.0022)	0.0004 (0.0035)	0.0037 (0.0030)
log(Num. Households) ₂₀₁₉	-0.0099* (0.0024)	0.0012 (0.0039)	0.0041 (0.0034)
$\Delta \log(\text{Num. Households})_{2019-2001}$	-0.0004 (0.0004)	0.0008 (0.0006)	0.0004 (0.0005)
$\Delta \log(\text{Business Establishments})_{2019-2000}$	-0.0011 (0.0005)	0.0003 (0.0007)	-0.0000 (0.0006)
College Share ₂₀₀₀	0.0000 (0.0002)	0.0001 (0.0003)	0.0005 (0.0002)
Foreign Share ₂₀₀₀	-0.0005* (0.0001)	0.0004 (0.0003)	0.0006 (0.0003)
Amenities Index	-0.0124* (0.0016)	-0.0039 (0.0020)	0.0033 (0.0018)

Notes: Each cell lists the slope coefficient (robust standard errors clustered at the two-digit zip code level in parentheses) from separate regressions of the form: $Y_i = \beta_0 + \beta_1 LU_i + \varepsilon_i$. The key right-hand-side variable in column 1 is zip code land unavailability, measured with a five percent buffer around each zip code polygon. Similarly, columns 2 and 3 use land unavailability measured at the three-digit and county levels, respectively, with a five percent buffer around each polygon. All LHS variables are aggregated to the zip code level. An asterisk represents statistical significance at the 1 percent level.

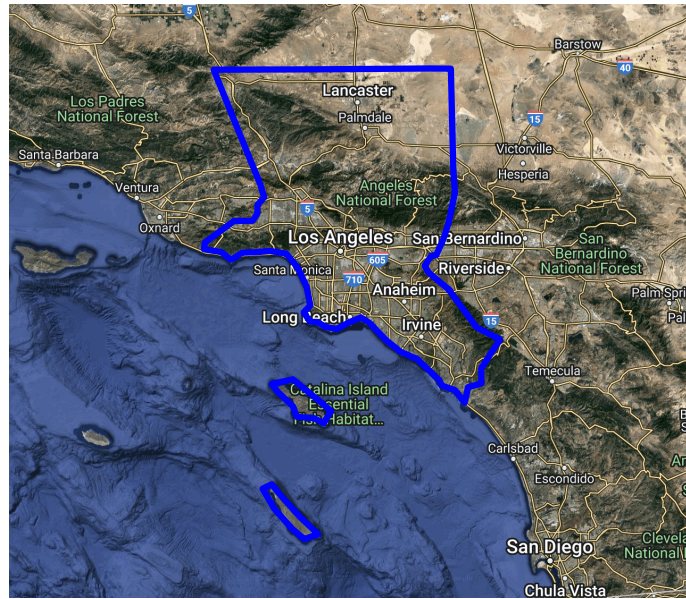
Figure 1: Saiz Land Unavailability Coverage for Los Angeles



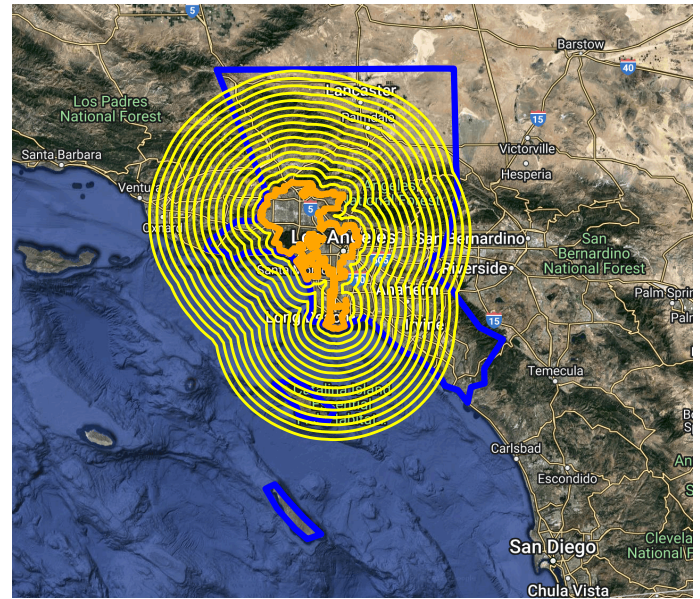
Notes: The blue line represents the polygon for the Los Angeles-Long Beach MSA using 1999 delineations. The orange lines signify the central cities within the Los Angeles MSA, and the red dots are the centroids for the central cities. The yellow circle has a radius of 50 kilometers and is centered around the polygon centroid for the first Los Angeles central city (Los Angeles).

Figure 2: LU Buffers and Circles for Los Angeles

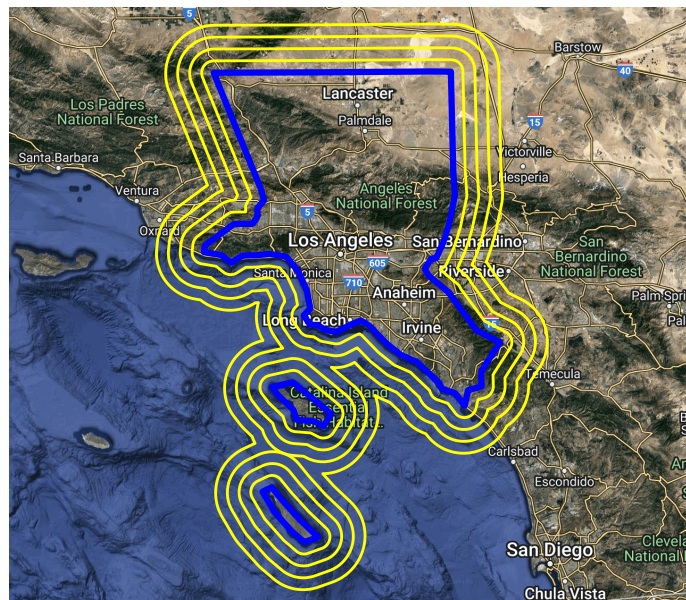
A: LA–Long Beach–Anaheim CBSA



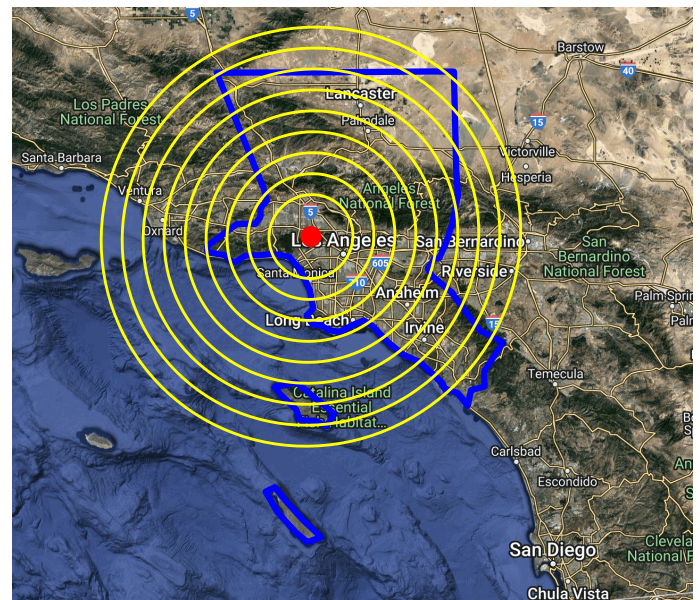
B: First Principal City Buffers



C: CBSA Polygon Buffers



D: First Principal City Centroid Circles

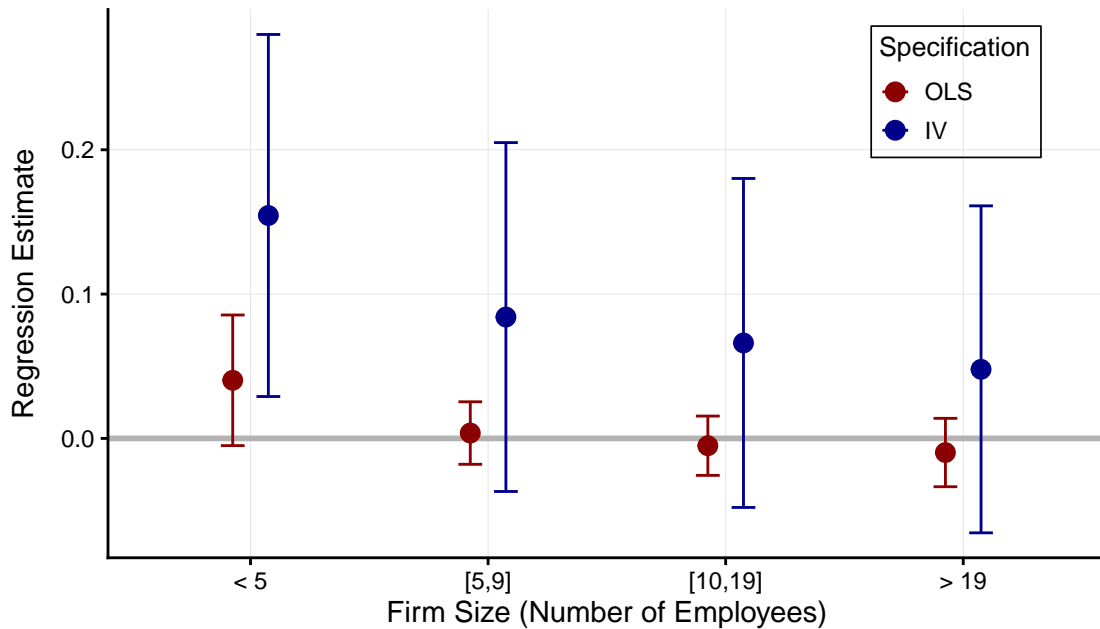


Notes: The blue line in all panels represents the polygon for the Los Angeles–Long Beach–Anaheim CBSA using 2015 delineations. Within each panel, the yellow lines represent the boundaries for which we calculate land unavailability. In panel B, the orange polygon signifies the first principal city (Los Angeles). The yellow lines correspond to 10 to 150 percent buffers (by 10 percentage point increments) of the first principal city polygon. Panel B shows 5 to 20 percent buffers (by 5 percentage point increments) of the CBSA polygon. The red dot in panel D is the principal city centroid. The corresponding yellow circles have a radius ranging from 20 to 100 kilometers (by 10 kilometer increments) centered at the first principal city centroid (red dot).

Figure 3: Pre-COVID-19 and COVID-19 Era House Price Growth and Firm Counts by Firm Size

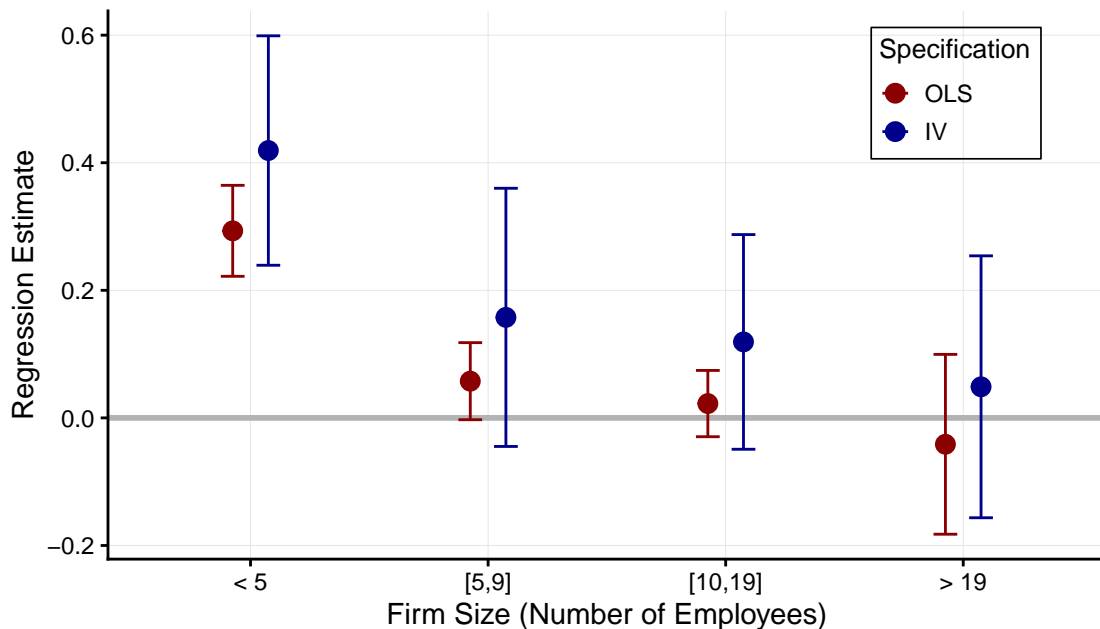
A: Pre-COVID-19 Period (2011Q1 - 2020Q1)

LHS: Number of Firms per Capita, YoY Log Difference;
 Endogenous Var: House Prices, YoY Log Difference;
 Instrument: LU-ML



B: COVID-19 Period (2020Q2 - 2022Q2); Difference Relative To Pre-COVID Period by Firm Size Category

LHS: Number of Firms per Capita, YoY Log Difference;
 Endogenous Var: House Prices, YoY Log Difference;
 Instrument: LU-ML



Notes: Error bands correspond to ± 2 robust standard errors clustered by county and year-quarter.

Figure 4: Florida 2001 Land Cover Dataset

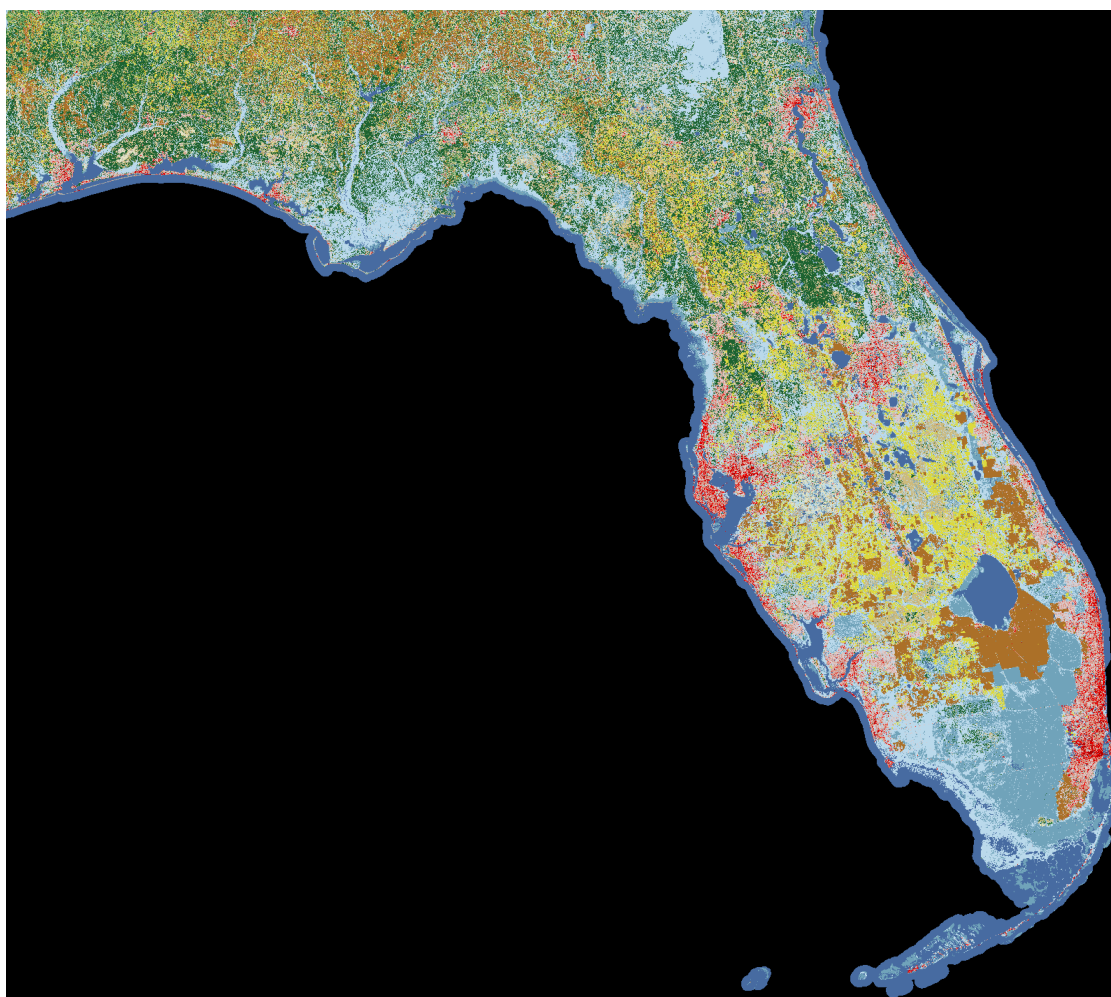
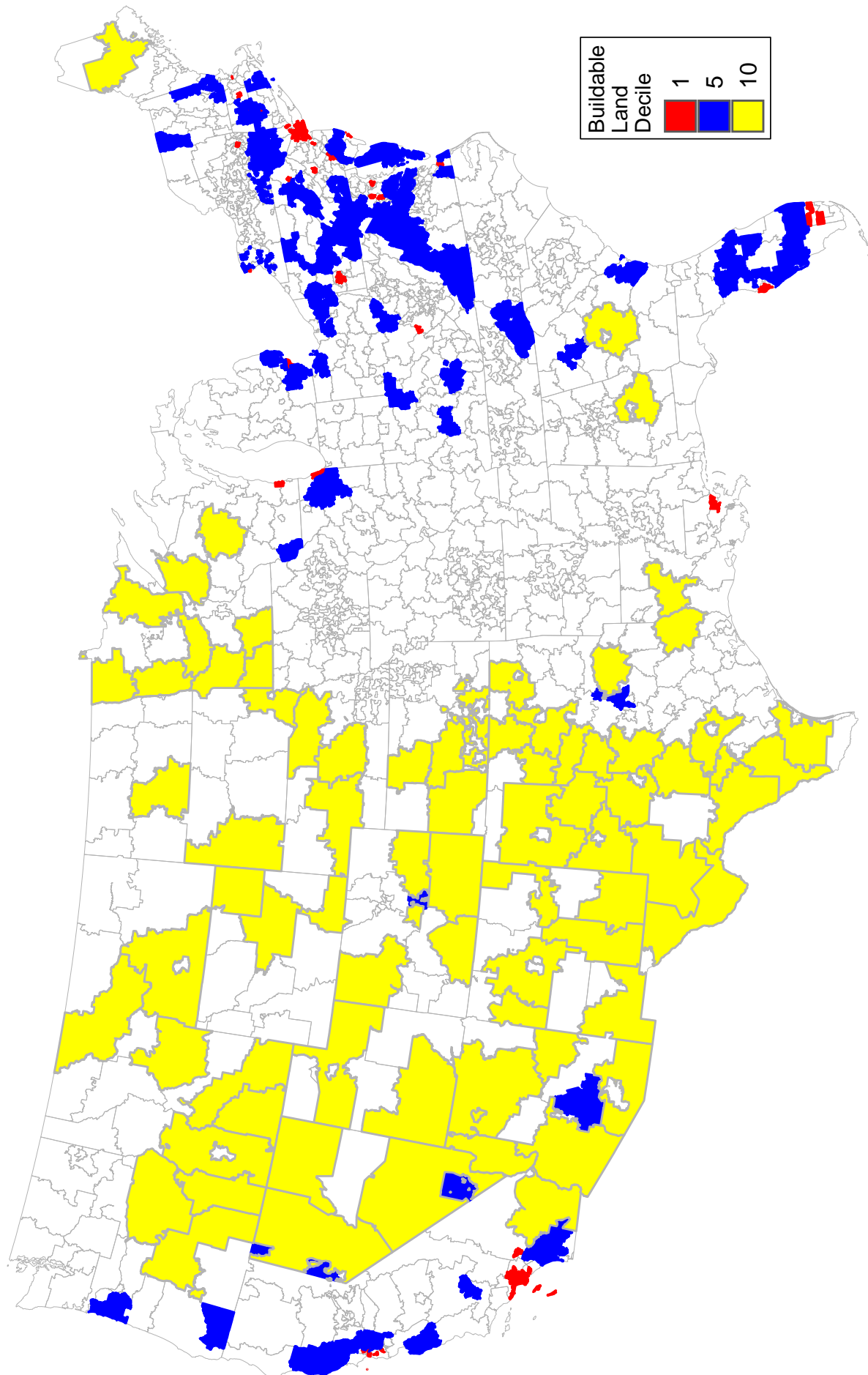
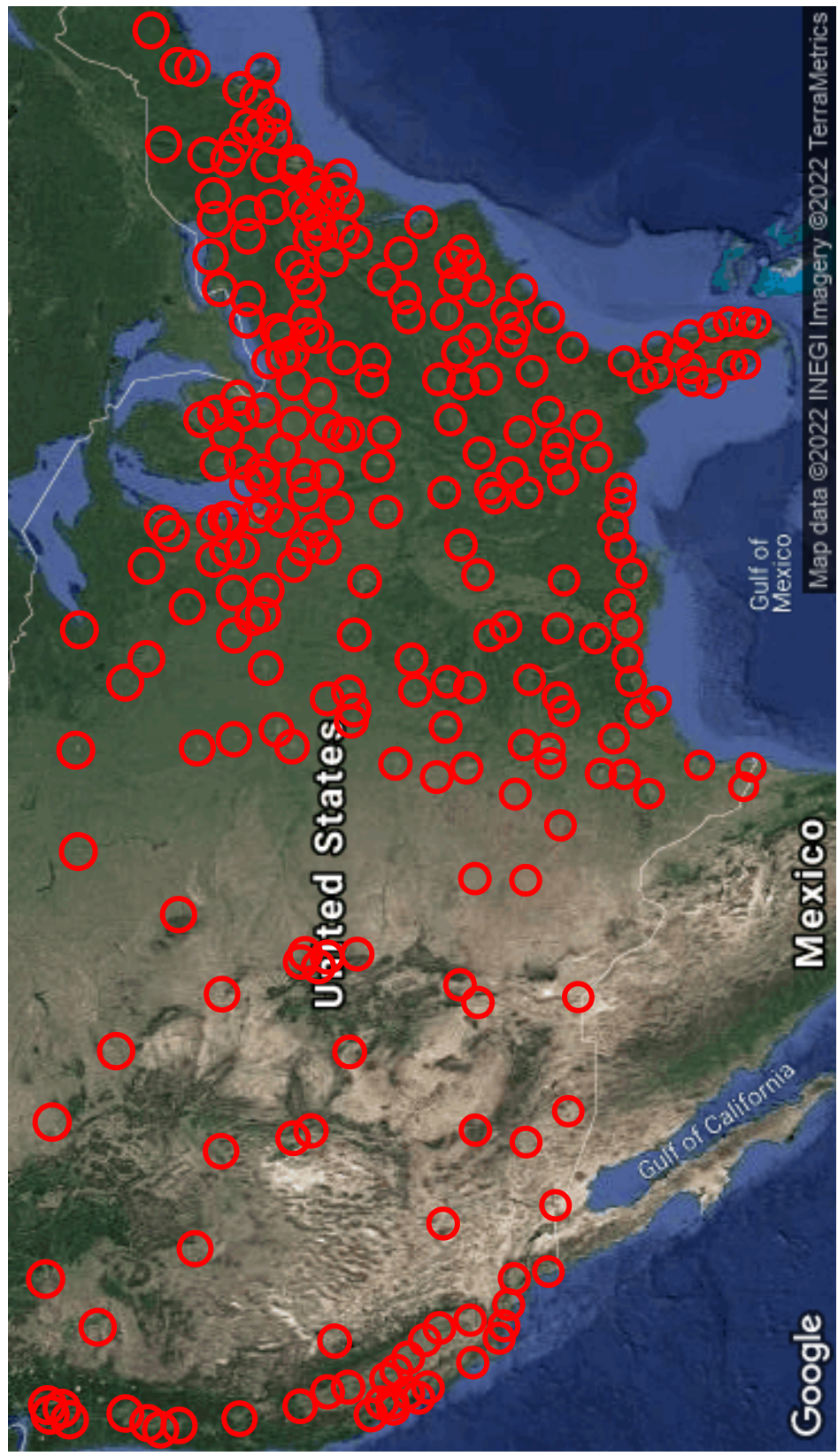


Figure 5: Three Digit Zip Codes and Buildable Land Deciles 1, 5, and 10



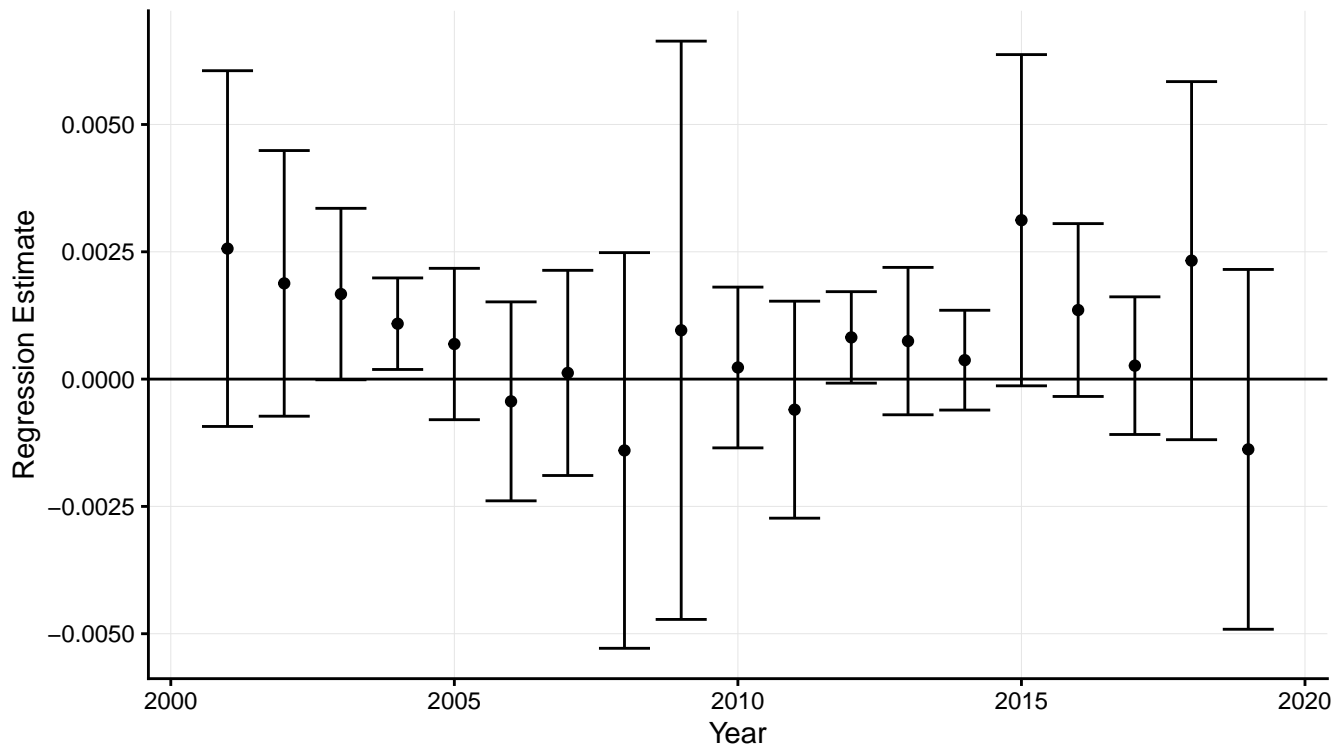
Notes: Three digit zip codes. Red areas are buildable land decile 1; blue areas are buildable land decile 5; and yellow areas are buildable land decile 10.

Figure 6: Saiz Land Unavailability Coverage for United States



Notes: Red circles have a radius of 50k km and are centered around the central city centroid of each MSA as in the [Saiz \(2010\)](#) dataset.

Figure 7: Annual Correlations between Bartik Shocks and LU



Notes: County-level correlations between LU and [Bartik \(1991\)](#) labor demand shocks are from the following model estimated separately by year: $Bartik_i = \alpha + \beta \cdot LU_i + \epsilon_i$. $Bartik_i$ represents the annual BLS QCEW Bartik shock for county i and LU is land unavailability for county i computed using a 5 percent buffer around each county polygon. Error bars correspond to ± 2 robust standard errors clustered at the state level.